UC Irvine

UC Irvine Previously Published Works

Title

Spatiotemporal variability of biogenic terpenoid emissions in Pearl River Delta, China, with high-resolution land-cover and meteorological data

Permalink

https://escholarship.org/uc/item/14n0x36m

Journal

Tellus B, 63(2)

ISSN

0280-6509

Authors

WANG, XUEMEI
SITU, SHUPING
GUENTHER, ALEX
et al.

Publication Date

2011-04-01

DOI

10.1111/j.1600-0889.2010.00523.x

Copyright Information

This work is made available under the terms of a Creative Commons Attribution License, availalbe at https://creativecommons.org/licenses/by/4.0/

Peer reviewed

eScholarship.org Powered by the California Digital Library
University of California

Tellus SERIES B CHEMICAL AND PHYSICAL METEOROLOGY
PUBLISHED BY THE INTERNATIONAL METEOROLOGICAL INSTITUTE IN STOCKHOLM

Tellus (2011), 63B, 241–254
Printed in Singapore. All rights reserved

© 2011 The Authors
Tellus B © 2011 John Wiley & Sons A/S

TELLUS

Spatiotemporal variability of biogenic terpenoid emissions in Pearl River Delta, China, with high-resolution land-cover and meteorological data

By XUEMEI WANG[1]*, SHUPING SITU[2], ALEX GUENTHER[3], FEI CHEN[3], ZHIYONG WU[1], BEICHENG XIA[1] and TIJIAN WANG[4], [1]*School of Environmental Science and Engineering, Sun Yat-sen University, Guangzhou 510275, China;* [2]*Guangzhou Research Institute of Environmental Science, Guangzhou 510620, China;* [3]*National Center for Atmospheric Research, CO, USA;* [4]*School of Atmospheric Science, Nanjing University, Nanjing 210093, China*

(Manuscript received 24 March 2010; in final form 13 December 2010)

ABSTRACT

This study intended to provide 4-km gridded, hourly, year-long, regional estimates of terpenoid emissions in the Pearl River Delta (PRD), China. It combined Thematic Mapper images and local-survey data to characterize plant functional types, and used observed emission potential of biogenic volatile organic compounds (BVOC) from local plant species and high-resolution meteorological outputs from the MM5 model to constrain the MEGAN BVOC-emission model. The estimated annual emissions for isoprene, monoterpene and sesquiterpene are 95.55×10^6 kg C, 117.35×10^6 kg C and 9.77×10^6 kg C, respectively. The results show strong variabilities of terpenoid emissions spanning diurnal and seasonal time scales, which are mainly distributed in the remote areas (with more vegetation and less economic development) in PRD. Using MODIS PFTs data reduced terpenoid emissions by 27% in remote areas. Using MEGAN-model default emission factors led to a 24% increase in BVOC emission. The model errors of temperature and radiation in MM5 output were used to assess impacts of uncertainties in meteorological forcing on emissions: increasing (decreasing) temperature and downward shortwave radiation produces more (less) terpenoid emissions for July and January. Strong temporal variability of terpenoid emissions leads to enhanced ozone formation during midday in rural areas where the anthropogenic VOC emissions are limited.

1. Introduction

This study utilizes high-resolution land-cover data, meteorological and biogenic emission models to provide 4 km × 4 km gridded, year-long estimates of the amount, spatial distribution and temporal variations of major biogenic volatile organic compounds (BVOC) in the Pearl River Delta (PRD) region, China. It represents the preliminary attempt to explore their diurnal and seasonal variations and their potential contributions to regional variability of surface ozone (O_3). Tropospheric ozone, known both as a greenhouse gas and for having adverse effects on human health, vegetation and materials, is formed by complex photochemical reactions involving NO_x and volatile organic compounds (VOC) precursors. Investigations have shown that up to 90% of the total VOC emissions are from biogenic sources (Guenther et al., 1995). In North America, BVOC emissions are estimated to be seven times larger than anthropogenic VOC (AVOC) emissions (Guenther et al., 2000). Furthermore, BVOC emissions are more reactive than AVOC (Carter et al., 1995; Stockwell et al., 1997), and many BVOC emissions also play a key role in secondary organic aerosol (SOA) formation and thus can impact radiative forcing and climate change.

Early studies suggested that BVOC emissions in urban areas contribute negligibly to ozone formation due to their relatively small ambient levels compared with AVOC concentrations (Altshuller, 1983). Nevertheless, later studies focusing on the role of naturally emitted VOC on surface ozone in North America (Sillman et al., 1990; Tao et al., 2003; Cortinovis et al., 2005; Li et al., 2007) and in Asia (Shao et al., 2000; Han et al., 2005; Wang et al., 2008) revealed that BVOC could enhance ozone formation in most investigated areas because they are more reactive than AVOC. Studies from Carter et al. (1995) revealed that reactivity of BVOC has two to three times that of their counterparts from gasoline combustion. Therefore, they

*Corresponding author.
e-mail: eeswxm@mail.sysu.edu.cn
DOI: 10.1111/j.1600-0889.2010.00523.x

Fig. 1. Map of the Pearl River Delta (PRD) and its location in China.

can affect air quality even when they are emitted at lower rates. The impacts of BVOC on ozone formation become more prominent in summer when both photochemical activity and BVOC emissions reach their peak (Tsui et al., 2009). Therefore, it is very important to accurately characterize BVOC emissions.

The PRD region (about 41 700 km^2), located at the centre of Guangdong Province in southern China, has experienced remarkable economic development and urbanization during the past two decades. Nine major cities in the PRD form a supercity cluster (Fig. 1) including Guangzhou (GZ), Dongguan (DG), Foshan (FS), Shenzhen (SZ), Zhuhai (ZH), Zhongshan (ZS), Jiangmen (JM), Huizhou (HZ) and Zhaoqing (ZQ). Hong Kong is 'the Hong Kong special administrative region of the People's Republic of China', which is not administratively considered as part of PRD. Hong Kong and PRD together are the PRD economic zone (PRDEZ). O_3 and particle matter are the major air pollution issues in the PRD, with the maximum hourly averaged ozone concentration exceeding 180 parts per billion (ppbv) in 2008 (the national standard is 100 ppbv in China) (Zhang et al., 2008). The anthropogenic emissions over the PRD have been estimated by Streets et al. (2003) and Guangdong Environmental Protection Bureau (http://www.gdepb.gov.cn), which provide useful information as air-quality model inputs for understanding the sources of air pollutants. However, the emission inventories described by those studies have not yet included BVOC emissions. Recently, Zheng et al. (2010) used the GloBEIS model to characterize BVOC emissions and their uncertainties in this region. Tsui et al. (2009) generated a BVOC emission inventory for Hong Kong based on measurements of thirteen Hong Kong tree species. These measurements were incorporated into the emission factors (EFs) used for this study. Guenther et al. (1995) estimated the global distribution of BVOC, based on coarse resolution land-cover and meteorological data (0.5-degree), and using the global-average EFs. As a result, the tremendous variability in the PRD land-cover and land-use (LULC) due to urbanization was not properly accounted for in those studies. For example, urbanization rates were approximately 45% during 1990 and 70% during 2006 in the PRD. Wang et al. (2007) investigated the impacts of rapid urbanization in the PRD on ozone concentrations and found surface ozone can change 4–15 ppbv due to meteorological variations. Therefore, the actual BVOC emission estimate may be considerably different from these 'global model' values. Recently, there have been a few localized attempts to measure BVOC EFs in the PRD (Hu et al., 2001; Klinger et al., 2002) and Hong Kong (Tsui et al., 2009), and to estimate BVOC emissions in the PRD (Hu et al., 2001; Yang et al., 2001), and China (Klinger et al., 2002; Tie et al., 2006). Wei et al. (2007) studied the impacts of BVOC on ozone episodes during a tropical storm in the PRD and found that BVOC can increase daytime ozone peak values by 38 ppbv. However, this study only focused on a specific period and there was no systematic, quantitative evaluation of the importance of BVOC on regional ozone formation in the PRD.

Therefore, to further quantify the potential role of BVOC in regional photochemical smog pollution in the PRD, we used the high-resolution LULC data and a full-year of meteorological data obtained from a mesoscale model for 2006 to drive the state of the science MEGAN (the Model of Emissions of Gases and Aerosols from Nature) model to estimate BVOC emissions, their spatial distribution and seasonal variability, and to discuss the implications for ozone formation. In addition, we assessed the influences of uncertainties in specifying EFs, LULC and meteorological conditions on model estimated BVOC emissions. Terpenoids (isoprene, monoterpenes and sesquiterpenes) are the only BVOC emissions considered in this study because they are the major contributors to total BVOC emissions (Guenther et al., 2000; Duhl et al., 2008) and have important impacts on atmospheric oxidants and SOA (Lack et al., 2004; Wiedinmyer et al.,

2006; Liao et al., 2007; Sakulyanontvittaya et al., 2008a,b). This paper is organized as follows: Section 2 describes the methodology including the MEGAN model and input data; Section 3 presents the calculated BVOC emissions, their seasonal and diurnal distributions and associated uncertainties. This includes an analysis of the implications of BVOC on ozone formation combining the modelled BVOC emissions with the observed O_3 concentrations in the region. Section 4 summarizes the findings of this paper.

2. Methodology

2.1 MEGAN model

The MEGAN model was recently developed as the next-generation emission model for biogenic emissions to estimate the net emission of gases and aerosols from terrestrial ecosystems into the atmosphere. Driving variables required to execute MEGAN include LULC data, meteorological data and atmospheric chemical compositions (Guenther et al., 2006). Recently MEGAN, as another biogenic emission option, has been coded to integrate with atmospheric chemistry and transport models such as the Weather Research and Forecast-chemistry model (WRF-Chem) and the Community Multi-scale Air Quality model (CMAQ) version 4.7. The MEGAN code, description and user's guide can be downloaded from http://acd. ucar.edu/~guenther/ MEGAN/ MEGAN.htm. Guenther et al. (2006) and Sakulyanontvittaya et al. (2008a,b) described MEGAN and investigated the sensitivity of MEGAN emission estimates to the monoterpene and sesquiterpene parameters used for the United States. MEGAN version 2.1 employs the multilayer canopy model described by Guenther et al. (2006), which can be used to investigate energy balance within the vegetation canopy by explicitly calculating leaf temperature and light on sunlit and shaded leaves. MEGAN version 2.1 was used to estimate terpenoid emissions in 2006 over the PRD region.

The MEGAN framework described by Guenther et al. (2006) spatially and temporally calculates biogenic emissions based on EFs, satellite-derived vegetative cover data and site-specific environmental conditions. Emission rates (E) are calculated based on the following equation:

$$E = \varepsilon\gamma\rho,$$

where ε is an EF that represents the net above-canopy emission rate expected at standard conditions; γ is a normalized emission activity factor that accounts for changes due to deviations of environmental variables from standard conditions; ρ is a normalized factor that accounts for variations in chemical production and loss within plant canopies compared to standard conditions. Here, we set ρ to a value of 1 which results in a constant canopy loss rate at about 0.95 for isoprene (e.g. Karl et al., 2004; Stroud et al., 2005). γ can account for effects of canopy environment, leaf age and soil moisture. The effect of soil moisture is assumed to be negligible in the PRD region, based on the results of Guenther et al. (2006), so

$$\gamma = \gamma_{\mathrm{CE}} \times \gamma_{\mathrm{age}},$$

where γ_{CE} is the factor associated with LAI, light and temperature variations and γ_{age} is the factor associated with leaf age. The model calculates hourly emissions for 20 compounds/compound classes (138 compounds totally), which can be grouped into various chemical mechanisms. The dynamical equations and lumping schemes for different chemical mechanisms can be found in Sakulyanontvittaya et al. (2008a,b). Several chemical mechanisms can be chosen for model output in the MEGAN post process. The SAPRC99 chemical mechanism was chosen for this study as an example, so that the 37 monoterpene species are grouped into one monoterpene class. 2-m temperature, 10-m wind speed, 2-m water vapour mixing ratio, surface pressure, and downward shortwave radiation at each horizontal grid point used for driving MEGAN were calculated from the fifth-generation non-hydrostatic Mesoscale Meteorological Model (MM5) version 3.7.4 developed by the Pennsylvania State University–National Center for Atmospheric Research. The input data of the MEGAN model will be described in the following sections.

2.2 PFTs and ε

Accurate estimation of BVOC emissions highly relies on the accurate description of LULC. MEGAN groups plant species and area coverages by plant functional types (PFTs) but each PFT has a specified plant species composition for a given ecoregion. Total emissions are the sum of emissions estimated for each PFT in a given grid cell. Four PFTs are considered in the MEGAN: broadleaf trees (BT), needle leaf trees (NT), shrubs and bushes (SB) and grasses and crops (GC). The model default PFTs distribution based on 1-km Moderate Resolution Imaging Spectroradiometer (MODIS) data in 2003 can be downloaded from http://cdp.ucar.edu/acd/megan. The default MEGAN 1-km MODIS PFT distribution is compared with a PFT-distribution based on local datasets obtained from three ways. One is from Thematic Mapper (TM) images for 2006 with 30-m resolution, which is the primary PFTs distribution. The second data set is from Guangdong Forestry Bureau, which collects the total vegetation coverage for each county and also identifies the dominant tree species and vegetation categories including BT, NT and SB. The third data set is from field surveys conducted by a team from the Department of Environmental Science at Sun Yat-sen University. The survey team made 50 visits to the places where the TM data differs from the Forestry Bureau statistic data, mainly in Huizhou, Jiangmen, Zhuhai and Guangzhou. Field survey results are used to justify the TM data and calibrate the TM images. More details about the ground survey can be found in Situ et al. (2009). The results (Fig. 2) showed BT is the most

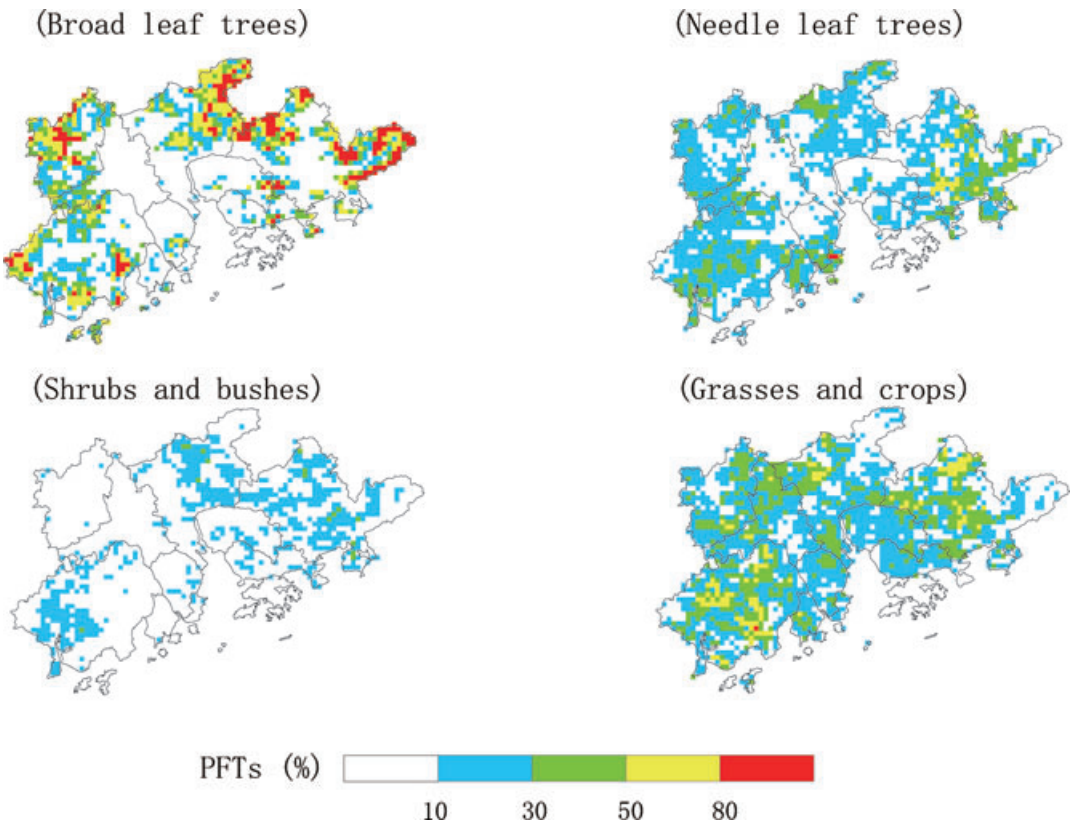

Fig. 2. Plant functional types (PFTs) distributions in the PRD.

dominant PFT in the PRD accounting for about 24.2% of total land-cover (about 12 043 km^2), followed by GC with 23.4% (about 11 645 km^2), NT with 18.0% (about 8929 km^2) and SB with 7.7% (about 3815 km^2). These PFT distributions were used as inputs to the MEGAN model.

Tsui et al. (2009) described the quantification of EFs for 13 Hong Kong tree species. Standard EFs of isoprene, total monoterpenes and the other VOCs were assigned to 148 Hong Kong tree species using the measurements of the thirteen tree species and other literature data (Tsui et al., 2009). PRD and Hong Kong share the same geographical region, and they have similar tree species and families, so Tsui et al. (2009) Hong Kong EFs were used for this study along with some other local measurements (Hu et al., 2001; Yang et al., 2001; Klinger et al., 2002; Wang et al., 2002; Zhao et al., 2004). The contributions of tree species in the PRD to the total tree cover of the area were used to weight and group the EFs for each PFT. The PFT distributions were used to calculate cell-based standard EFs in the PRD as shown in Table 1. The values within the parentheses are the model default values for global average EFs that were used to investigate the impacts of EFs on emissions in 3.2.1. Because there is no local measurement reported for sesquiterpene emission rates, the ratio of local studied EFs to global averaged EFs for monoterpene was used to generate sesquiterpene EFs. These estimates are within the range of values used in other studies (e.g. Wiedinmyer et al., 2000; Hu et al., 2001; Yang et al., 2001; Klinger et al., 2002; Wang et al., 2002; Yan et al., 2005; Sakulyanontvittaya et al., 2008b; Zheng et al., 2010).

2.3. *Meteorological variables from MM5*

Although land cover plays a key role in determining BVOC emissions, meteorological variables are also important inputs for the MEGAN model. MM5 was used to calculate the weather parameters with 12-km and 4-km grid spacing. Figure 3 shows these two domains and topographic distribution. The parameterization schemes used are Medium Range Forecast (MRF) PBL scheme and the NCAR Community Climate Model (CCM2) longwave and shortwave schemes and an explicit microphysical scheme that predicts rain, snow, graupel, cloud water and cloud ice for all domains. The Kain-Fritsch cumulus parameterization scheme was used for the outermost domain (D1), whereas no cumulus parameterization scheme was used for the finest domain (D2) because it was assumed that convection is reasonably well resolved by the explicit microphysics. A more detailed description can be found in Wang et al. (2007). MM5 was run for the whole year of 2006, and each run is for 5 days with 1-day spin-up time which is continuous run as described in Lin et al. (2007). The MEGAN model was run in D2 and the BVOC emissions in the PRD were estimated.

Table 1. Local-measurement based (model default global averaged) standard emission factors for BVOCs estimate in MEGAN (μg m^{-2} h^{-1})

PFT	Broadleaf trees	Needleleaf trees	Shrubs and bushes	Grasses and crops
BVOC				
ISO	5200 (13000)	800 (2000)	3850 (11000)	140 (400)
MYRC	53.6(20)	180.9(75)	51.6(22)	0.7(0.3)
SABI	88.8(45)	124.3(70)	86.3(50)	1.2(0.7)
LIMO	155.5(45)	311.1(100)	157.3(52)	2.1(0.7)
3CAR	56.6(18)	453.0(160)	68.8(25)	0.8(0.3)
OCIM	96.3(90)	57.8(60)	79.6(85)	0.9(1.0)
PINB	320.3(90)	960.9(300)	311.4(100)	4.7(1.5)
PINA	396.0(180)	891.1(450)	385.0(200)	3.9(2.0)
OMTP	189.4(90)	340.9(180)	202.6(110)	8.8(4.8)
FARN	58.4(35)	45.1(30)	43.8(30)	0.7(0.5)
BCAR	45.6(30)	82.1(60)	59.9(45)	1.2(0.9)
OSQT	143.5(75)	189.4(110)	142.3(85)	2.3(1.4)

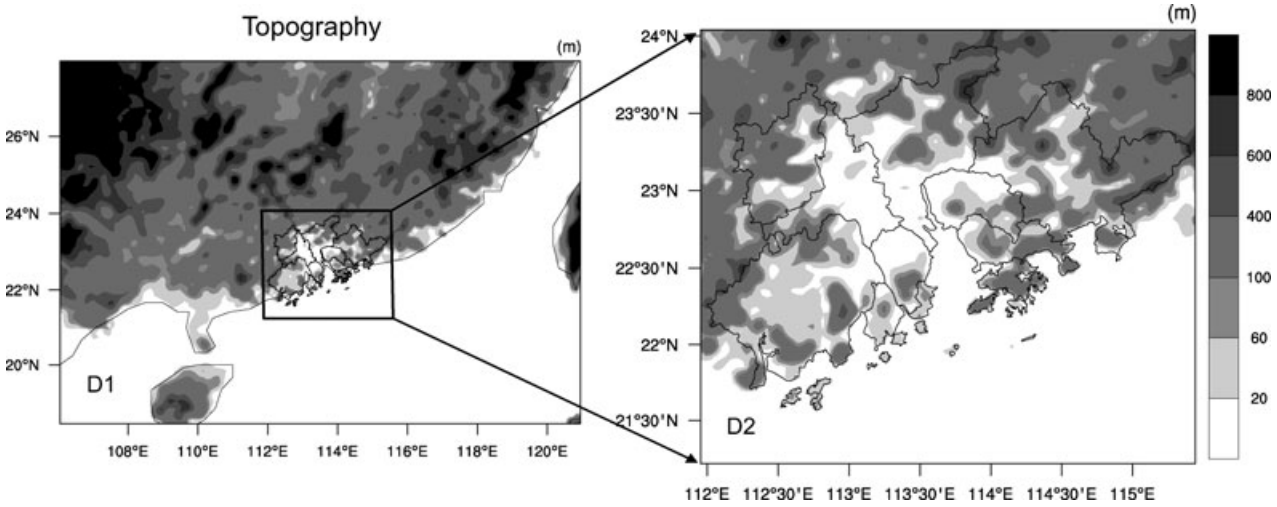

Fig. 3. MM5 modelling domains and topography. Domain 1 (D1): 12-km grid spacing; Domain 2 (D2): 4-km grid spacing.

Available weather data at 22 monitoring sites (such as Guangzhou, Shenzhen, Huizhou, Jiangmen, Guangning, Foshan, etc.) for January, April, July and October were used to validate the MM5 simulations in D2. Table 2 shows the verification statistics of MM5 simulated daytime 2-m temperature and downward shortwave radiation, including their root mean square errors (RMSEs) and mean absolute errors (MAEs). Simulated daytime 2-m temperature has a cold bias of 0.10, 0.14 and 0.66 °C for January, July and October, respectively; whereas in spring, simulated daytime 2-m temperature has a warm bias of 1.04 °C. Their RMSEs are generally less than 2 °C except for April. Simulated downward shortwave radiation is larger than the observation, probably due to the fact that MM5 does not take aerosol into account in absorbing and scattering solar radiation as noted by other studies (e.g. Chen and Dudhia, 2001). The maximum bias of downward shortwave radiation is 148 W m^{-2} for spring. MAEs of relative humidity for January, April, July and October are 9.1%, 9%, 7% and 7.5%, respectively. The annual mean observed relative humidity for the wet season (March to August) is 76.2% and the dry season (September to February) is 65.6%. Field experiments have shown that temperature and radiation can explain most of observed BVOC emission variability, so the sensitivity of model results to temperature and radiation RMSE will be discussed in Section 3.2.3. Overall, the meteorological conditions generated by MM5 are reasonably good for driving MEGAN.

Precipitation can indirectly influence BVOC emission in several ways including the impacts on shortwave radiation and leaf temperature, leaf phenological changes including LAI and leaf age, and through soil moisture. The MEGAN soil moisture algorithm is used only to decrease emissions during drought conditions. Because drought did not occur in the PRD during this simulation, we did not include the MEGAN soil moisture algorithm. Precipitation is a major driver of the

Table 2. Verification statistics of MM5 simulations at 22 surface monitoring sites

Variables	Period	Mean		Bias	MAE	RMSE
		Obs	Sim			
Daytime T2m (°C)	January	16.27	16.37	−0.10	1.55	1.97
	April	25.23	24.18	1.04	1.94	2.56
	July	29.57	29.72	−0.14	1.46	1.89
	October	26.37	27.03	−0.66	1.34	1.72
Daytime SWDOWN (W m^{-2})	January	247.9	284.5	36.6	97.30	126.9
	April	221.7	369.9	148.2	150.60	178.4
	July	272.8	330.5	57.7	96.78	115.8
	October	277.2	387.7	110.5	116.48	132.2

T2m: temperature at 2 m; SWDOWN: downward shortwave radiation; mean: mean value; Obs: observation; Sim: simulation; MAE: mean absolute error; RMSE: root mean square error.

environmental parameter γ_{age}, which is represented as $\gamma_{age} = F_{new}A_{new} + F_{gro}A_{gro} + F_{mat}A_{mat} + F_{old}A_{old}$. $A_{new}, A_{gro}, A_{mat}, A_{old}$ are the relative emission rates assigned to new leaves, growing leaves, mature leaves and old leaves, respectively. The values of these EFs are based on observations, which were summarized by Guenther et al. (2006), A_{new}(0.05), A_{gro} (0.6), A_{mat} (1.125), A_{old} (1). The canopy is divided into leaf age fraction based on the change in LAI between the current time step and the previous step, which implies the effects of precipitation.

3. Results and discussion

3.1. Seasonal and diurnal distributions

The control case was run for the whole year of 2006. Figure 4 presents the BVOC estimates over four typical months. Figure 4a indicates that the isoprene emissions calculated by MEGAN over the PRD show considerable spatial and interannual variations. They are the lowest in January but increase in April due to the increase in both temperature and incoming solar radiation. As temperature and solar radiation increases further in July, the isoprene emissions reach their annual maximum values. In October, the isoprene emissions start to decrease due to lower temperature and radiation. Note that throughout the year, the isoprene emissions are the highest in northeastern Guangzhou, Huizhou, Zhaoqing and Jiangmen, where broadleaf trees are dominant. The seasonally accumulated isoprene emissions are 4.31×10^6 kg C, 19.69×10^6 kg C, 45.73×10^6 kg C and 25.82×10^6 kg C for winter (DJF), spring (MAM), summer (JJA) and fall (SON), respectively, with a total annual value of 95.55×10^6 kg C in the PRD. The ratio of biogenic isoprene emissions between summer and winter is very large (about 10.6)

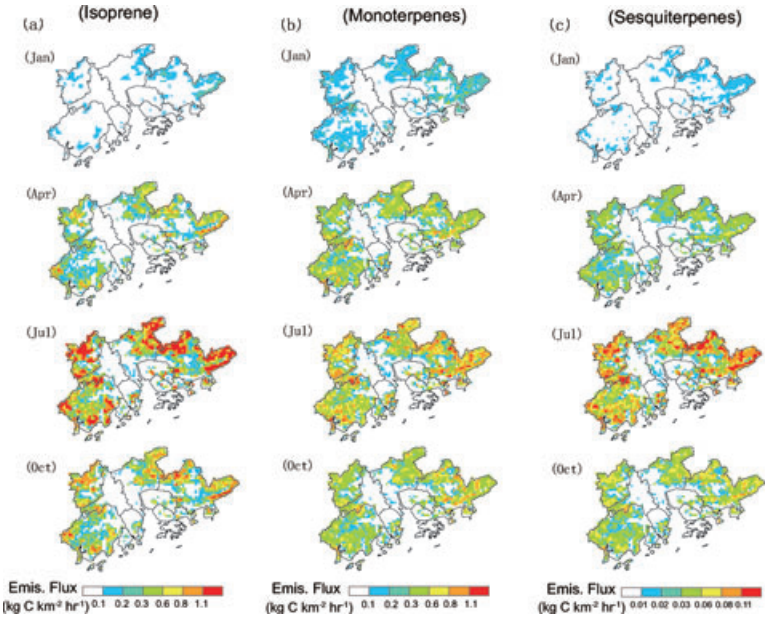

Fig. 4. Calculated biogenic emissions of (a) isoprene, (b) monoterpenes and (c) sesquiterpenes in January, April, July and October.

Table 3. Averaged BVOC emission flux (ton C km^{-2} per season or per year) estimated by MEGAN

Country/region	Area ($\times 10^4$ km^2)	Average period	Isoprene	MT	SQT	Reference
PRD	4.97[a]	Spring	0.396	0.568	0.042	This study
		Summer	0.920	0.858	0.092	This study
		Fall	0.520	0.600	0.053	This study
		Winter	0.087	0.336	0.010	This study
		Annual	1.923	2.361	0.197	This study
PRD	4.70	Annual	1.362	1.894		Zheng et al. (2010)
Hong Kong	0.11	Annual	2.364	3.091		Tsui et al. (2009)
Beijing	1.80	Annual	0.889	0.222		Wang et al. (2003)
China	960	Annual	0.423	0.361		Klinger et al. (2002)
			0.802	0.329		Tie et al. (2006)
North America	2400	Annual	1.221	0.746		Guenther et al. (2000)
Global (land)	14680	Annual	3.426	0.865		Guenther et al. (1995)

[a]Calculated areas using model grids.

under control case. The impacts of the meteorological variables RMSE on emissions will be studied in Section 3.2.3.

Table 3 shows the MEGAN-estimated seasonally averaged isoprene emissions. The fluxes fall between 0.087 and 0.920 ton C km^{-2}, whereas the reported mean isoprene-emissions for all of China falls between 0.02 and 0.53 ton C km^{-2} per season (Tie et al., 2006). The isoprene emissions in the PRD region are higher than the average value for Beijing and of the whole China because the PRD region has a higher vegetation coverage (37%) compared with Beijing (7%) and the whole China (14%). The higher BVOC emissions in the PRD were also due to the higher temperature and radiation. The PRD seasonal amplitude is smaller compared with the China averaged value (27) because of smaller annual variations of temperature and radiation in the PRD. Our results are higher than Zheng et al.'s (2010), whose results are 64×10^6 kg C in the PRD. Zheng et al. (2010) also indicated that the relative error for isoprene is -82% to $+177\%$, ranging from 10.87×10^6 to 163.42×10^6 kg C. Our results fall within this range. Eighty-six automatic meteorological monitoring stations data were used in Zheng et al.'s (2010) study to interpolate in 16 720 grids which may lower the temperature and radiation, although in this study, the radiation simulations from MM5 are higher than the observation data which can lead to higher isoprene emissions. On the other hand, the chemical production and loss factor ρ was set to 1 in this study but was 0.96 in Zheng et al. (2010). Yang et al. (2001) only estimated emissions for several tree species in the PRD, so the emissions are lower as expected. Area-averaged isoprene emissions in the PRD are lower than Hong Kong because Hong Kong has a higher vegetation rate (41%) (Tsui et al., 2009) than PRD (37%).

The spatial distribution of monoterpene emissions is different from that of isoprene emissions (Fig. 4b), especially in southern Huizhou where needle leaf trees are dominant, which have higher EFs of monoterpenes than broadleaf trees (Table 1). The seasonal variations of monoterpene emissions follow a pattern similar to isoprene. The seasonally accumulated monoterpene emissions are 16.68×10^6, 28.23×10^6, 42.64×10^6 and 29.80×10^6 kg C for winter, spring, summer and fall, respectively, with a total annual value of 117.35×10^6 kg C that is higher than the emissions of isoprene. The ratio of biogenic monoterpene emissions between summer and winter is about 2.6, indicating a smaller seasonal variation than that of isoprene. This is because monoterpene emissions are sensitive to changes in temperature and light. Because the PRD is located in the subtropical area, the seasonal variation of temperature is small and the averaged difference of temperature between July and January is 13.3 °C, compared to the value of 26.9 °C between summer and winter in Beijing. Table 3 shows the monoterpene emissions fall between 0.336 and 0.858 ton C km^{-2} per season, whereas the averaged monoterpene emissions for all of China fall between 0.02 and 0.19 ton C km^{-2} per season (Tie et al., 2006). Zheng et al. (2010) reported a monoterpene emission in the PRD of 68×10^6 kg C, which is lower than our result. The uncertainty analysis showed that the uncertainty ranges from 49.9×10^6 to 102.22×10^6 kg C (Zheng et al., 2010). The main reason for this difference is that our EFs for monoterpene are higher than Zheng et al.'s (2010). In this study, monoterpene was a group representing 37 species, mainly sabinene, limonene, myrcene, α-pinene and β-pinene. The dominant monoterpene species are α-pinene and β-pinene, which account for 55% of the total emissions.

The spatial distribution of sesquiterpene emissions is similar to the monoterpene emissions (Fig. 4c), but their emission amount is smaller. The calculated sesquiterpene emissions are 0.49×10^6, 2.08×10^6, 4.57×10^6 and 2.63×10^6 kg C in winter, spring, summer and fall respectively, with a total annual value of 9.77×10^6 kg C. The highest emission occurs in summer responding to the highest temperature and incoming solar radiation. The ratio of biogenic sesquiterpene emissions between summer and winter is about 9.3. The sesquiterpene emissions in the PRD are about 10 times lower than monoterpene and isoprene.

Table 4. Relative contribution of each PFT to BVOC emissions (%)

	BT	NT	SB	GC
Isoprene	74.4	7.14	16.9	1.58
Monoterpenes	32.8	57.3	9. 6	0.35

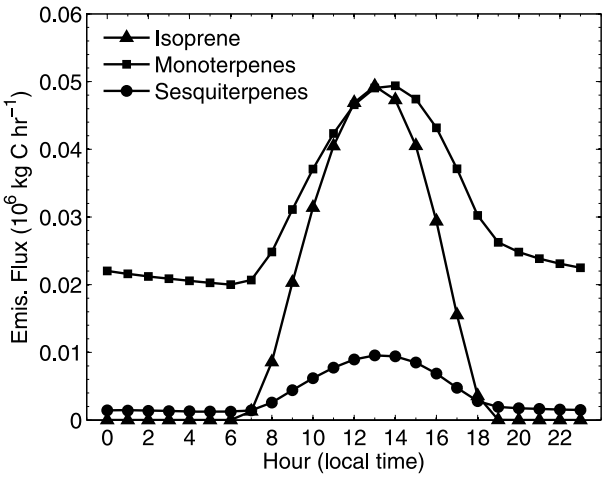

Fig. 5. Diurnal variation of terpenoids emission.

Figure 4 shows that the distribution of monoterpene emissions is different from that of isoprene emissions, which is largely due to PFT distributions. As shown in Table 1, different PFTs have different EFs for isoprene, monoterpenes and sesquiterpenes. To identify the relative contributions of each PFT to BVOC emissions, a number of sensitivity experiments have been conducted in which EFs for one particular PFT was used while the EFs of other PFTs were set to zero. Because the emissions in July are the highest, results from these runs for July are shown in Table 4. Broadleaf trees are the biggest contributor to isoprene emissions (about 74.4% of total isoprene emissions) and shrubs are the second largest contributor to isoprene emissions (about 16.9% of total isoprene emissions). Needle leaf trees are the biggest contributor to monoterpene emissions, about 57.3% of monoterpene emissions; broadleaf trees have the second highest contribution to monoterpene emissions in the PRD, about 32.8% of monoterpene emissions.

In addition, there is a strong diurnal variation in biogenic emissions. Figure 5 shows the annual average diurnal variation of biogenic emissions of isoprene, monoterpenes and sesquiterpenes over the area. In general, biogenic emissions are highest at 1300 local standard time (LST) and lowest at night, whereas Tie et al. (2006) showed the highest emissions averaged for the whole China at 1200 LST. Such a difference is due to the location of the PRD in subtropics, which usually have the highest temperature and solar radiation shortly after local noontime. The isoprene emissions have the largest diurnal variability among BVOC. During noontime, the isoprene emissions reach a maximum, and are then quickly reduced in the afternoon around 1800 LST. At night, the isoprene emissions are negligible in the absence of solar radiation. The monoterpene emissions are not zero at night because some monoterpene emissions are not dependent on downward radiation, leading to a smaller diurnal variability for monoterpenes than for isoprene. The ratio of the monoterpene emissions between noontime and nighttime is about 2.2. Sesquiterpene emissions have the same diurnal variation as monoterpene emissions. The ratio of the sesquiterpene emissions between noontime and nighttime is about 6.6.

3.2. *Uncertainties associated with PRD terpenoid emissions*

As we have described, BVOC emissions can be influenced by a number of factors including PFTs, LAI, meteorological conditions, EFs, foliar density and the algorithms relating emissions to these driving variables. Simulated BVOC emissions are hence subject to considerable uncertainties associated with these inputs and relationships. For instance, Guenther (1997) used six land-cover data sets to estimate potential emission variation in United States and found a three- to five-fold difference in estimated inherent emission capacity. The range of uncertainties for Beijing BVOC estimates is also very large, ranging from 50% to 100% (Wang et al., 2003). Zheng et al. (2010) quantified BVOC emission uncertainties in the PRD using the Monte Carlo method. The results indicated that EFs and model empirical coefficients were the key uncertainty sources for isoprene emissions whereas EFs and foliar density were the key uncertainty sources for monoterpenes and other BVOC. Potential sources of uncertainty include a lack of process understanding, and a resulting over simplification of processes, representation of heterogeneous vegetation with a limited number of PFTs, uncertain model parameters and uncertainty in driving variables such as meteorological data (Gulden et al., 2008). However, here we focus only on uncertainties that result from EFs, PFT distributions and meteorological variables.

Three sensitivity experiments were performed to assess the impacts of PFTs, surface meteorological variables and EFs on BVOC emissions. The detailed experimental design is presented in Table 5. Compared to the control simulation we have discussed so far, the first sensitivity experiment no. 1 used global-averaged EFs, sensitivity experiment no. 2 used global MODIS PFTs distributions and sensitivity experiment no. 3 explores the uncertainties in meteorological variables. The global average EFs are provided as the MEGAN model default options.

3.2.1. Impacts of EFs on emission estimates. In the first sensitivity experiment, global default EFs (EFs) were used to assess the impacts of EFs on emission estimates. Table 1 shows EFs which come from the model default option [global averaged EFs (in parentheses)] and the regional EFs (control run) developed for this study. Generally, isoprene EFs are lower in this study

Table 5. Experiment design for sensitivity tests

Experiment	Control	1	2	3
PFTs	TM and ground survey derived	TM and ground survey derived	MODIS	TM and ground survey derived
EFs	This study	Global average	This study	This study
Meteorology	MM5	MM5	MM5	Modified MM5

whereas monoterpene and sesquiterpene EFs are much higher than global-averaged values. Compared with the control run, the BVOC emission distribution pattern does not change due to the same PFT distribution. The total BVOC emissions using global-averaged EF values in the PRD are higher than this study, about 24% higher for the control run, because of higher isoprene EFs. The results showed that total isoprene emissions using the default global-averaged values are 2.5 times higher than the estimated values for the control run, whereas the total amount of monoterpene and sesquiterpene emissions is reduced by about 42% compared with the values of the control run. The ratio of isoprene to total BVOC is 65% in the simulation using global averaged EFs and 32% in the control run. The ratio of combined monoterpene and sesquiterpene emissions to total BVOC is less than 15% under global averaged EFs, while for the control run, the ratio is about 42%. Global-averaged EFs tend to increase the total BVOC emissions in the PRD by augmenting isoprene emissions even though there is a reduction in monoterpene and sesquiterpene emissions. Because monoterpenes and sesquiterpenes have higher SOA formation yields, lower estimation of terpenes will reduce SOA formation in the PRD, whereas the higher isoprene emission estimates will produce higher model ozone estimates in the PRD.

3.2.2. Impact of PFT distribution on emission estimates. A global PFT database based on MODIS was used to investigate the impacts of PFT distributions on emission estimates in the second sensitivity experiment. The MODIS PFTs data in the PRD represents the year of 2003 in the model default option, while in the control run the PFT data is for 2006. The interannual variability between 2003 and 2006 is usually small and its effect can be ignored. Figure 6 shows the PFT distributions with the MODIS PFTs data. There are significant differences between the MODIS PFTs data and our TM and local-survey data used in the control simulation for spatial distribution and density of vegetation (Fig. 2). MODIS PFTs data show that the dominant PFT in the PRD is GC with coverage of 45.3%, followed by NT, SB and BT with coverage of 21.8%, 18.0% and 1.9%, respectively. As a result of this major difference in PFT classification, the spatial distribution and amount of terpenoid emissions were substantially altered. Figure 7 shows the difference in emissions between the control simulation and the sensitivity simulation using MODIS PFTs. Terpenoid emissions decreased 27% in the PRD with the spatial difference. In the central PRD, terpenoid emissions increased mainly in south GZ, FS, DG and SZ, which is VOC-control area (Zhang et al., 2008), the maximum amount of isoprene and monoterpene emissions increased more than 100 g C km^{-2} h^{-1} and sesquiterpene emission increased more than 10 g C km^{-2} h^{-1}. More BVOC emissions in these areas will enhance ozone and SOA formation. The amount of terpenoid emissions decreased in the remote areas in the PRD, such as HZ, JM and the north of GZ. Among the terpenoids, isoprene emissions have the largest decrease by 49% compared with the control simulation because BT coverage is lower with the MODIS PFTs data.

3.2.3. Impact of meteorological variables on emission estimates. As discussed earlier, temperature and downward shortwave radiation are the main meteorological parameters influencing BVOC emissions. Hence, in the third sensitivity experiment, we chose January and July to conduct the sensitive study, because July (January) has the highest (lowest) BVOC emissions. In the sensitivity simulations, we perturb the daytime temperature and solar radiation by their RMSE for each time step during the MEGAN model execution as following:

$$T = T_0 \pm \mathrm{RMSE},$$

$$R = R_0 \pm \mathrm{RMSE},$$

where T and R are the input temperature and downward shortwave radiation to drive the MEGAN model; T_0 and R_0 are the values from the MM5 simulation output from 0800 to 1800 LST; RMSE is taken from verification statistics in Table 2. Average simulated temperature for July (January) is 29.72 °C (16.37 °C), and the RSME is 1.89 °C (1.97 °C). Average simulated downward shortwave radiation for July (January) is 330.5 W m^{-2} (284.5 W m^{-2}) and the RSME is 115.8 W m^{-2} (126.9 W m^{-2}).

Four sensitivity studies were conducted to investigate the impacts of meteorological variables on BVOC emissions. Table 6 shows the daytime (0800–1800 LST) relative changes of terpenoid emissions for different sensitivity studies. As expected, increasing (decreasing) temperature and downward shortwave radiation produces more (less) terpenoid emissions for July and January, of which isoprene emission ranges from −19.2% to +26.7% due to temperature variations and −39.6% to +50.7% due to radiation variations, monoterpene emission ranges from −18.5% to +16.2% due to temperature variations and −14.3 to +16.8% due to radiation variations and sesquiterpene emission ranges from −18.6% to +24.2% due to temperature variations and −16.3% to +20.8% due to radiation variations. Temperature change in January produces a larger impact on isoprene

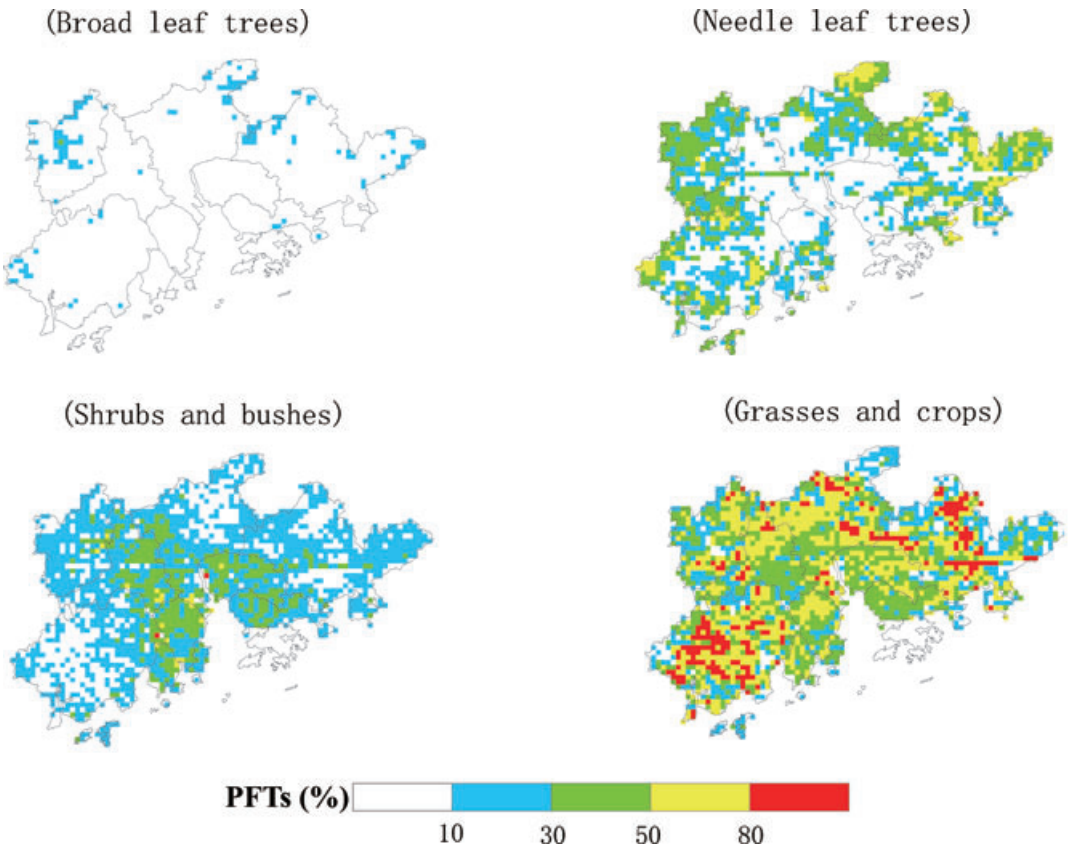

Fig. 6. Plant functional types (PFTs) distribution with MODIS data.

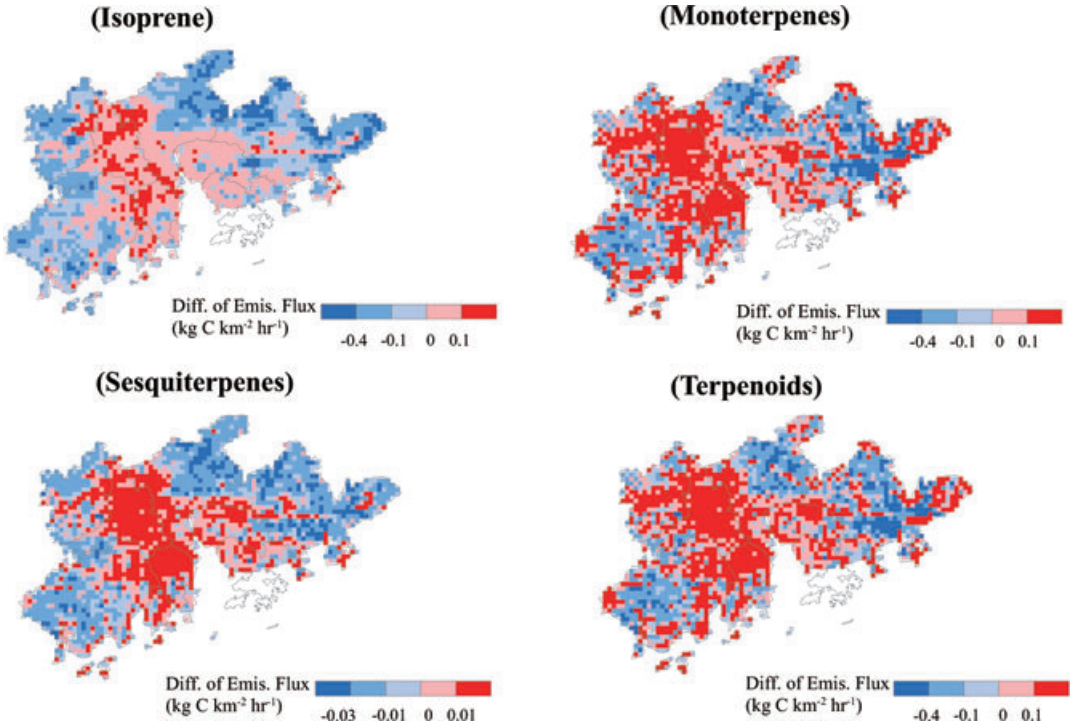

Fig. 7. Differences of emission flux (emissions estimated with the MODIS PFTs minus emissions estimated with local-survey PFTs).

Table 6. Relative changes of BVOC emissions under different temperature and radiation (%)

	Isoprene		Monoterpenes		Sesquiterpenes	
	July	January	July	January	July	January
Increase temperature	23.6	26.7	16.2	11.9	23.6	24.2
Decrease temperature	−19.2	−21.7	−18.5	−10.0	−18.5	−18.6
Increase radiation	36.2	50.7	16.8	5.8	16.8	20.8
Decrease radiation	−31.4	−39.6	−14.3	−4.6	−14.3	−16.3

emissions than that in July, while its impact on monoterpene emissions is reversed as compared with isoprene. Sesquiterpenes emission changes due to temperature change are almost similar in both July and January. Variations in emissions due to modifying downward shortwave radiation have the same trend as with modifying temperature. Isoprene emissions occurring during daytime are more sensitive to radiation. Monoterpene emissions are more sensitive to temperature in January, while in July monoterpene emissions depend on both temperature and downward shortwave radiation. Sesquiterpene emissions are sensitive to both temperature and downward shortwave radiation in July and January.

3.3. The implication of BVOC emissions for ozone formation

Wang et al. (2005) showed that a simulation with the STEM (Sulfur Transport and dEposition Model) can underestimate the ozone concentration in the PRD. An underestimation of BVOC emissions by the coarse resolution GEIA global BVOC emissions database, used in Wang et al. (2005), could be an important reason. The higher BVOC emission amount calculated in this study with high-resolution input variables and the MEGAN model could improve the representation of the role of BVOC emissions for ozone formation in this region. Thus, it is important to compare BVOC emissions to AVOC emissions to shed some light on the implication of BVOC emissions on ozone formation in the PRD.

Figures 8a and b show the distribution of annual averaged AVOC and BVOC emissions in the PRD respectively. The AVOC emissions are obtained from Zheng et al. (2009) based on 2006 inventory data. The annual averaged AVOC emissions in the PRD are 8.3×10^5 ton yr^{-1}, and the BVOC emissions are 3.4×10^5 ton yr^{-1}. The ratio of the BVOC emissions to the AVOC emissions is 0.4 in the PRD, while the ratio for all of China is 0.7 (Tie et al., 2006). Although this ratio might suggest a relatively small influence of BVOC emissions for the whole PRD region compared with AVOC, a comparison of emissions at different locations within the PRD shows that BVOC emissions can dominate in some areas. The highest AVOC emissions are mostly in the central PRD mega cities, such as southern GZ, FS, DG and SZ, which are more developed districts with high industrial activity and high-density population. By contrast, BVOC emissions are highest in densely forested areas, such as northern GZ, HZ, ZQ and JM. BVOC can play important roles in ozone formation in particular locations, including areas where the BVOC emissions are higher than AVOC emissions. To address this issue, Figs 8a and b show the location of areas with significant AVOC and BVOC emissions (<1.2 kg km^{-2} h^{-1}). They indicate that the areas with significant AVOC emissions have almost no overlap with significant BVOC emissions. As a result, BVOC and NO can play important roles in the remote areas and could lead to substantial enhancement of ozone concentrations. Comparing Figs 8b and d, it can be seen that the co-location of anthropogenic sources of NO_x with higher biogenic sources of reactive VOC in the remote areas, particularly isoprene, can generate large amounts of ozone as shown in Fig. 8c. For example, the average ozone is higher around HZ where there is substantial BVOC emission and at the same time relatively lower AVOC and NO_x emissions. Figure 8c is the annual averaged surface ozone concentration distribution in the PRD based on an interpolation of the observation data. There are 13 air-quality monitor sites in the PRD and three sites in Hong Kong (http://www-app.gdepb.gov.cn/EQPublish/raqi.aspx). Hourly concentrations of SO_2, NO_2, PM_{10} and O_3 have been observed. It shows the regions with the highest ozone concentrations, such as HZ and north GZ, have higher BVOC emissions than AVOC emissions, indicating that BVOC emissions could play an important role for enhancing ozone production in the developing region over the PRD. FS and southern GZ are the lowest ozone concentration areas. Similar to AVOC emissions (Fig. 8a), the highest anthropogenic NO_x emissions (Fig. 8d) are located in FS, southern GZ, DG and SZ. The highest anthropogenic NO_x emissions titrate ozone in those areas and lead to the lowest ozone concentrations. In HZ and northern GZ, the highest ozone concentrations are associated with high BVOC emissions and relatively low NO_x emissions.

Differences in the spatial distributions of AVOC and BVOC emissions can potentially enhance the ozone concentration in the remote region. The strong temporal variability of BVOC emissions is another important factor in determining the importance of its implication in ozone formation. Observational studies in the PRD region show that ozone production is highest around 1400 LST, resulting from the strong photochemical activities at

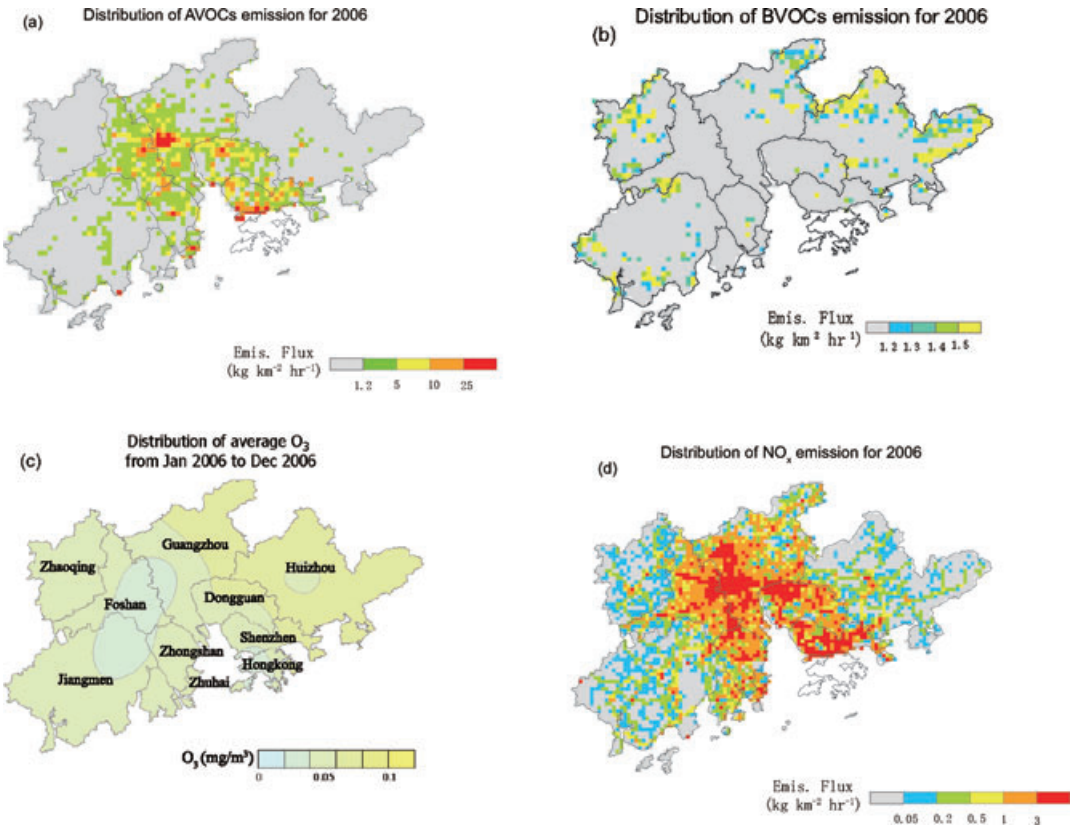

Fig. 8. (a) AVOC emission flux, (b) BVOC emission flux, (c) annual average O_3 concentration and (d) anthropogenic NO_x emission flux for 2006. *Source:* (a,d) From Zheng et al. (2009) and (c) from http://www-app.gdepb.gov.cn/EQPublish/raqi.aspx.

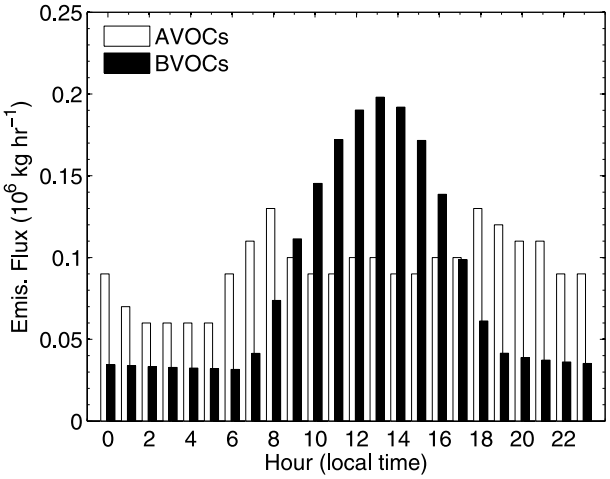

Fig. 9. Diurnal cycles of the BVOC emissions (dark bars) and the AVOC emissions (white bars) in July over the PRD.

that time (Shao et al., 2009). Figure 9 shows the diurnal variation of the BVOC emissions and the AVOC emissions in July. There are two peaks of the AVOC emissions, one is at 0800 LST and the other is at 1800 LST. Wang et al. (2005) found that 68% of the AVOC emissions come from transportation, therefore, the diurnal variation of the AVOC emissions roughly corresponds to rush hour traffic. The BVOC emissions calculated for this study are significantly larger than AVOC emissions during the daytime. At 1300 LST, the peak of the BVOC emissions and when the rate of ozone formation is the highest, the ratio of the BVOC emissions to AVOC emissions is about 1.4. This result indicates that even though the annual total BVOC emissions is lower than the annual total AVOC emissions in the PRD, the BVOC emissions play an important role in controlling ozone formation due to large spatial and temporal variations.

4. Summary and conclusions

The MEGAN version 2.1 was used to simulate terpenoid emissions (mainly isoprene, monoterpenes and sesquiterpenes) in the PRD for the whole year of 2006. Meteorological variables from MM5 model simulations with 4 × 4-km-grid spacing, such as 2-m temperature, downward shortwave radiation and 10-m wind speed and humidity, were used to drive MEGAN. The results show strong variability of terpenoid emissions spanning diurnal and seasonal time scales. The highest terpenoid emissions are in July around local noon, whereas the lowest emissions are in January during night due to lower temperature and solar radiation. Monoterpene emissions have smaller

seasonal variations than isoprene. Total annual isoprene, monoterpene and sesquiterpene emissions are 95.55×10^6, 117.35×10^6 and 9.77×10^6 kg C, respectively. These annual amounts are higher than the area-averaged values for China, largely due to denser forests and a warmer climate in the PRD. Broadleaf trees are the biggest contributor to isoprene emissions, about 74.4%; shrubs are the second largest contributor to isoprene emissions, about 16.9%; needle leaf trees are the biggest contributor to monoterpene emissions, about 57.3%, broadleaf trees have the second highest contribution to monoterpene emissions in the PRD.

Sensitivity studies were conducted to characterize the uncertainties associated with EFs, PFT distributions and meterological variables. The results show that (1) using the default global-average EFs in MEGAN produces more BVOC, by about 24%, producing 1.5 times more isoprene but less monoterpene and sesquiterpene, by about 42%. (2) BVOC emission distributions are sensitive to the PFT distributions used to model simulations. The results show that terpenoid emissions decreased by 27% when using MODIS 2003 PFTs data, in comparison to the high-resolution data developed for this study, mainly within remote areas. (3) increasing (decreasing) temperature and downward shortwave radiation produces more (less) terpenoid emissions. Under temperature variations (RSME), emissions change from -19.2% to $+26.7\%$, -18.5% to $+16.2\%$ and -18.6% to $+24.2\%$ for isoprene, monoterpenes and sesquiterpenes, respectively. Under radiation variations (RSME), emissions change from -39.6% to $+50.7\%$, -14.3% to $+16.8\%$ and -16.3% to $+20.8\%$ for isoprene, monoterpenes and sesquiterpenes, respectively.

Although annual BVOC emissions are lower than AVOC emissions (40%), significant spatial and temporal variations in BVOC emissions make them more dominant at some locations and times, and could lead to enhanced ozone formation. The higher BVOC emissions (>1.2 kg km^{-2} h^{-1}) occur in rural regions where AVOC emissions are relatively low and ozone concentrations are the highest in the PRD. Because of strong seasonal and diurnal variations, biogenic VOC emissions are significantly larger than anthropogenic VOC emissions during the daytime in July when the rate of ozone production in the PRD is the highest.

This study presents initial results indicating that BVOC emissions in the PRD may be important for ozone formation. Future work will quantitatively investigate the impacts of BVOC emissions on ozone formation using a three-dimensional atmospheric chemical and transport model.

Acknowledgments

This research was supported by the NSFC projects (U0833001, 40875076) and the US NCAR BEACHON (Bio-hydro-atmosphere interactions of Energy, Aerosols, Carbon, H_2O, and Organics and Nitrogen) Program. This was supported by the National Program on Key Basic Research Project of China (973) under Grant Nos. 2010CB428504 and 2010CB428503 and also supported by National High Technique Research and Development Program (863) 2 0 0 6 A A 0 6 A 3 0 7.

References

Altshuller, A. P. 1983. Review: natural volatile organic substances and their effect on air quality in the United State. *Atmos. Environ.* **17**(11), 2131–2165.

Carter, W., Pierce, J., Luo, D. and Malkina, I. 1995. Environmental chamber study of maximum incremental reactivities of volatile organic compounds. *Atmos. Environ.* **29**(18), 2499–2511.

Chen, F. and Dudhia, J. 2001. Coupling an advanced land-surface/hydrology model with the Penn State/NCAR MM5 modeling system. Part I: Model implementation and sensitivity. *Mon. Wea. Rev.* **129**, 569–585.

Cortinovis, J., Solmon, F., Serca, D., Sarrat, C. and Rosset, R. 2005. A simple modelling approach to study the regional impact of a Mediterranean forest isoprene emission on anthropogenic plum. *Atmos. Chem. Phys.* **5**, 1915–1929.

Duhl, T. R., Helmig, D. and Guenther, A. B. 2008. Sesquiterpene emissions from vegetation: a review. *Biogeosciences.* **5**, 761–777.

Guenther, A. 1997. Seasonal and spatial variations in natural volatile organic compound emissions. *Ecol. Appl.* **7**, 34–45.

Guenther, A., Hewitt, C., Erickson, D., Fall, R., Geron, C. and co-authors. 1995. A global model of natural volatile organic compound emissions. *J. Geophys. Res.* **100**, 8873–8892.

Guenther, A., Geron, C., Pierce, T., Lamb, B., Harley, P. and co-authors. 2000. Natural emissions of non-methane volatile organic compounds, carbon monoxide, and oxides of nitrogen from North America. *Atmos. Environ.* **34**, 2205–2230.

Guenther, A., Karl, T., Harley, P., Wiedinmyer, C., Palmer, P. and co-authors. 2006. Estimates of global terrestrial isoprene emissions using MEGAN (Model of Emissions of Gases and Aerosols from Nature). *Atmos. Chem. Phys.* **6**, 3181–3210.

Gulden, L. E., Yang, Z. L. and Niu, G. Y. 2008. Sensitivity of biogenic emissions simulated by a land-surface model to land cover representations. *Atmos. Environ.* **42**, 4185–4197.

Han, Z. W., Ueda, H. and Matsuda, K. 2005. Model study of the impact of biogenic emission on regional ozone and the effectiveness of emission reduction scenarios over eastern China. *Tellus.* **57B**, 12–27.

Hu, Y. T., Zhang, Y. H., Xie, S. D. and Zeng, L. M. 2001. Development of biogenic VOC emissions inventory with high temporal and spatial resolution. *China Environ. Sci.* **22**(6), 1–6.

Klinger, L. F., Li, Q. J., Guenther, A., Greenberg, J. and co-authors. 2002. Assessment of volatile organic compound emissions from ecosystems of China. *J. Geophys. Res.* **107**(21), ACH 16–19.

Lack, D., Tie, X. X., Bofinger, N., Wiegand, A. and Madronich, S. 2004. Seasonal variability of atmospheric oxidants due to the formation of secondary organic aerosol: a global modeling study. *J. Geophys. Res.* **109**, doi:10.1029/2003JD003418.

Li, G. H., Zhang, R., Fan, J. and Tie, X. X. 2007. Impacts of biogenic emissions on photochemical ozone production in Houston, Texas. *J. Geophys. Res.* **112**(D10309), doi:10.1029/2006JD007924.

Liao, H., Henze, D. K., Seinfeld, J. H., Wu, S. L. and Mickley, L. J. 2007. Biogenic secondary organic aerosol over the United State:

comparison of climatological simulations with observations. *J. Geophys. Res.* **112**, doi:10.1029/2006JD007813.

Lin, W. S., Sui, C.-H., Yang, L. M., Wang, X. M. and co-authors. 2007. A numerical study of the influence of urban expansion on monthly climate in dry autumn over the Pearl River Delta, China. *Theor. Appl. Climatol.* **89**, doi: 10.1007/s00704-006-0244-6.

Sakulyanontvittaya, T., Duhl, T., Wiedinmyer, C., Helmig, D., Matsunaga, S. and co-authors. 2008a. Monoterpene and sesquiterpene emission estimates for the United States. *Environ. Sci. Technol*. **42**, 1623–1629.

Sakulyanontvittaya, T., Guenther, A., Helmig, D., Milford, J., Milford, J. and co-authors. 2008b. Secondary organic aerosol from sesquiterpene and monoterpene emissions in the United States. *Environ. Sci. Technol.* **42**, 8784–8790.

Shao, M., Zhao, M., Zhang, Y., Peng, L. and Li, J. 2000. Biogenic VOCs emissions and its impact on ozone formation in major cities, China. *J. Environ. Sci. Health Part A Environ. Sci. Eng.* **35**, 1941–1950.

Shao, M., Zhang, Y. H., Zeng, L. M., Tang, X. Y., Zhang, J. and co-authors. 2009. Ground-level ozone in the Pearl River Delta and the role of VOCs and NO_x in its production. *J. Environ. Manage*. **90**, 512–518.

Situ, S. P., Wang, X. M., Guenther, A., Cai, Z. W. and Deng, R. R. 2009. Typical summertime isoprene emission from vegetation in the Pear River Delta region, China. *China Environ. Sci.* **29**(4), 822–829.

Stockwell, W., F. Kirchner and F. Kuhn. 1997. A new mechanism for regional atmospheric modelling. *J. Geophys. Res.*, **102**, 25847–25879.

Stroud, C., Makar, P., Karl, T., Guenther A. and co-authors. 2005. Role of canopy-scale photochemistry in modifying biogenic-atmosphere exchange of reactive terpene species: results from the CELTIC field study. *J. Geophys. Res.,* **110**, doi:10.1029/2005JD005775.

Sillman, S., Logan, J. A. and Wofsy, S. C. 1990. The sensitivity of ozone to nitrogen oxides and hydrocarbons in regional ozone episodes. *J. Geophys. Res*. **95**, 1837–1851.

Streets, D. G., Bond, T. C., Carmichael, G. R., Fernands, S. D., Fu, Q. and co-authors. 2003. An inventory of gaseous and primary aerosol emissions in Asia in the year 2000. *J. Geophys. Res.* **108**(D21), 8809, doi:10.1029/2002JD003093.

Tao, Z. N., Larson, S. M., Wuebbles, D. J., Willams, A. and Caughey, M. 2003. A summer simulation of biogenic contributions to ground level ozone over the continental United States. *J. Geophys. Res*. **108**(D14), 4404, doi:10.1029/2002JD002945.

Tie, X., Li, G., Ying, Z., Guenther, A. and Madronich, S. 2006. Biogenic emissions of isoprenoids and NO in China and comparison to anthropogenic emissions. *Sci. Total Environ.* **371**, 238–251.

Tsui, J., Guenther, A., Yip, W. K. and Chen, F. 2009. A biogenic volatile organic compound emission inventory for Hong Kong. *Atmos. Environ.* **43**: 6442–6448, doi:10.1016/j.atmosenv.01.027.

Wang, Q. G., Han, Z. W., Wang, T. J. and Zhang, R. J. 2008. Impacts of biogenic emissions of VOC and NO_x on tropospheric ozone during summertime in eastern China. *Sci. Total Environ.* **395**, 41–49.

Wang, X. K., Mou, Y. J., Ouyang, Z. Y., Zhang, X. S., Ni, S. F. and co-authors. 2002. Study on emission of isoprene from major plants living in Taihu Ba sin. *Chin. Bull. Botany* **19**(2), 224–230.

Wang X. M., Carmichael, G., Chen, D. L., Tang, Y. H. and Wang, T. J. 2005. Impacts of different emission sources on air quality during March 2001 in the Pearl River Delta (PRD) region. *Atmos. Environ.* **39**(29), 5227–5241.

Wang, X. M., Lin, W. S., Yang, L. M., Deng, R. R. and Hui, L. 2007. A numerical study of influences of urban land-use change on ozone distribution over the Pearl River Delta Region, China. *Tellus B* **59B**, 633–641.

Wang, Z. H., Bai, Y. H. and Zhang, S. Y. 2003. A biogenic volatile organic compounds emission inventory for Beijing. *Atmos. Environ.* **37**(27), 3771–3782.

Wei, X. L., Li, Y. S., Lam, K. S., Wang, A. Y. and Wang, T. J. 2007. Impact of biogenic VOC emissions on a tropical cyclone-related ozone episode in the Pearl River Delta region,China. *Atmos. Environ.* **41**, 7851–786.

Wiedinmyer, C., Strange, I. W., Estes, M., Yarwood, G. and Allen, D. T. 2000. Biogenic hydrocarbon emission estimates for North Central Texas, *Atmos. Environ.* **34**, 3419–3435.

Wiedinmyer, C., Tie, X., Guenther, A. 2006. Changes in biogenic volatile organic emissions that occur as a result of land cover change: how do they affect regional and global atmospheric chemistry? *Earth Interact* **10**:1–19.

Yan, Y., Wang, Z. H., Bai, Y. H., Xie, S. D. and Shao, M. 2005. Establishment of vegetation VOC emission inventory in China. *China Environ. Sci.* **25**(1), 110–114.

Zhang, Y. H., Su, H., Zhong, L. J., Cheng,Y. F., Zeng, Y. F. and co-authors. 2008. Regional ozone pollution and observation-based approach for analyzing ozone–precursor relationship during the PRIDE-PRD2004 campaign. *Atmos. Environ.* **42**(25), 6203–6218.

Zhao J, Bai, Y. H., Wang, Z. H. and Zhang, S. Y. 2004. Studies on the emission rates of plants VOCs in China. *China Environ. Sci.* **24**(6), 654–657.

Zheng, J. Y., Zhang, L. J., Che, W. W. and co-authors. 2009. A highly resolved temporal and spatial air pollutant emission inventory for the Pearl River Delta Region, China and its uncertainty assessment. *Atmos. Environ.* **43**(32), 5112–5122.

Zheng, J. Y., Zheng, Z. Y., Yu, Y. F., Zhong, L. J. 2010. Temporal, spatial characteristics and uncertainty of biogenic VOC emissions in the Pearl River Delta area. *Atmos. Environ.* **44**, 1960–1969.

Yang, D. J., Bai, Y. H., Li, J. L., Pan, N. M., Yu, K. H. and co-authors. 2001. Study on hydrocarbon compounds from natural source in Pearl River Delta area. *China Environ. Sci*. **21**(50), 422–426.